Temperature dependence of the magnetoresistance of sputtered Fe/Cr superlattices

J. E. Mattson, Mary E. Brubaker, C. H. Sowers, M. Conover, Z. Qiu, and S. D. Bader
Materials Science Division, Argonne National Laboratory, Argonne, Ilinios 60439
(Received 19 April 1991)

The temperature dependence of the resistivity of three sputtered Fe/Cr superlattices was analyzed. Two are antiferromagnetic and one is ferromagnetic. Also, a series of Fe/Cr superlattices was characterized as a function of Cr thickness by means of resistivity, Kerr-rotation, and x-ray-diffraction measurements. Magnetoresistance measurements for films with 32-Å Fe layers confirm the presence of three oscillations with peaks at ~11, 27, and 42 Å Cr. The Kerr-rotation measurements for fixed Fe thicknesses of 15, 25, 32 and 40 Å indicate that the first antiferromagnetic region is always between ~6 and 17 Å Cr thickness. The low-angle x-ray results show that the structure is not ideal, based on comparison to dynamical simulation or to the quality of similarly prepared Fe/Mo superlattices. The magnetoresistivity of the antiferromagnetic films decays from its maximum value at low temperature with a T^2 behavior below ~100 K, while a ferromagnetic film could be similarly approximated by a $T^{3/2}$ behavior. These power laws are a consequence of the thermal excitation of magnons in these anisotropic antiferromagnetic and ferromagnetic superlattices, respectively. The resistivities due to *sd*-interband scattering ρ_{sd} are approximated by a T^2 behavior and roughly a T^3 behavior, respectively. This indicates that for the antiferromagnetic films the dominant contributions to ρ_{sd} come from processes mediated by magnons as well as phonons.

I. INTRODUCTION

The properties of Fe/Cr superlattices are of great current interest because they exhibit exotic magnetic coupling and magnetoresistive behavior. In 1986 Grünberg, *et al.*[1] discovered that ferromagnetic Fe layers can couple *antiferromagnetically* across intervening, ultrathin Cr layers. Subsequently a *giant magnetoresistance* was discovered.[2] It has also been observed that the coupling in sputtered films oscillates between ferromagnetic and antiferromagnetic (AF) with increasing thickness of the intervening Cr layers.[3] these developments have stimulated widespread experimental and theoretical interest. The essential issues are to understand the nature of both the AF ground state and the spin-dependent scattering mechanisms which give rise to the giant magnetoresistance (MR). The systems that show oscillatory magnetic coupling now include Fe/Cr, Co/Ru, Co/Cr (Ref. 3), Fe/Cu (Refs. 4 and 5), Co/Cu (Ref. 6), and Fe/Mo (Ref. 7), and the list is growing. RKKY-type interactions (Rudeman-Kittel-Kasuya-Yosida) have been explored theoretically to understand the oscillatory magnetic behavior,[8] and the transport properties have been modeled microscopically and macroscopically.[9,10] Camley and Barnas[9] suggested that the temperature dependence of the MR could be attributed to the variation of the mean free path. In the present work, we study the temperature dependence of the MR experimentally and find strong correlation between the MR and the excitation of magnons. We also confirm the findings of Parkin, More, and Roche[3] that the magnitude of the MR oscillates as a function of the Cr thickness for sputtered Fe/Cr superlattices.

The paper is organized as follows: In Sec. II we provide experimental background material, including an x-ray structural characterization of representative Fe/Cr superlattices. In Sec. III A we present magneto-optic Kerr-rotation results to demonstrate that the films are well behaved and that the sign of the magnetic coupling varies as a function of Cr thickness. In the remainder of Sec. III we map out a methodology for analyzing the MR. Section III B contains MR results versus Cr thickness, and Sec. III C contains MR results versus temperature for two AF films and one ferromagnetic film. In Sec. IV the temperature-dependent results are discussed in terms of the thermal population of magnons. Also, the remaining contributions to the resistivity are found to be amenable to conventional analysis. Finally, Sec. V summarizes the main observations and conclusions of the work.

II. EXPERIMENTAL BACKGROUND

The films were grown in a Microscience chamber using dc magnetron sputtering from two diode guns. The chamber was turbo-pumped to an ultimate base pressure of 2×10^{-9} Torr after a mild bake out at 90 °C. The argon pressure during evaporation was 3 m Torr, and deposition rates of 5 Å/s were monitored by quartz-crystal oscillators mounted above each gun. Polished sapphire substrates were cleaned, then loaded through a load-lock into the evaporation chamber. The deposition process utilized a computer-controlled stepping motor to move

the sample alternately over each sputtering target. Target materials of 99.9% nominal purity were used.

The samples consisted of a series of films, each with a constant Fe-layer thickness but varying Cr thicknesses. Films with an Fe thickness of 32 Å all contained 30 bilayers. However, films with Fe thicknesses of 15, 25, and 40 Å contained 20 bilayers for the thinnest bilayer films, 15 bilayers for thicker films, and 10 bilayers for the thickest films. This was to keep the total film thickness nominally greater than about 500 Å so that substrate effects in the optical measurements are negligible.

Low-angle and high-angle x-ray-diffraction measurements were performed on these films with a Rigaku θ-2θ diffractometer using 1 kW of Cu $K\alpha$ radiation. The high-angle scans show that the films are [110]-textured, and the rocking curves are very broad. The low-angle measurements [Figs. 1(a) and 1(c)] show the characteristic peaks associated with the layering in the films and allow for a direct measurement of the bilayer thickness. Comparison of the experimental data in Fig. 1(a) with the dynamical simulation[11] in Fig. 1(b) suggests that the interfaces are intermixed over a number of atomic layers. We draw this conclusion by noting that the higher-order diffraction peaks do not appear for the thinnest Cr layers. Also note that one can see in Fig. 1(b) the expected destructive interference in the second and third peaks as the ratio of the Cr-to-Fe thickness changes. The x-ray data show that though there may be considerable variation in the crystallographic orientation, as indicated by the broad, high-angle rocking curves, the films are, nonetheless, layered, as indicated by the low-angle data. By contrast, results for Fe/Mo (Ref. 7) superlattices grown similarly in the same apparatus show the full richness of diffraction peaks anticipated from simulation.

The longitudinal Kerr rotation is measured using p-polarized light by monitoring the change in intensity of the reflected light due to the polarization rotation caused by the magneto-optic interaction. There are no mechanical adjustments of the optical components during measurements. The difference in the measured light intensity ΔI upon magnetic-field reversal, normalized to the average intensity is $|\Delta I/\bar{I}| \approx 4\Phi_K/\delta$, where δ is the angle of the analyzer polarization axis from extinction (typically set to $\approx 1°$). The Φ_K values are obtained from the ΔI values taken from the hysteresis loops in either the remnant state or the saturation state.

Longitudinal MR measurements (with applied magnetic field **H** parallel to the current) have been made both as a function of Cr-layer thickness (for constant Fe thickness) and as a function of temperature T for selected films. The samples were first masked (using photolithography and chemical etching in concentrated H_2SO_4) into a standard, four-terminal, bar geometry. Since the films are polycrystalline in the plane of the film, no care was taken to orient the direction of the current (or mask) with respect to the substrate. The temperature-dependent measurements were performed using ac (20 Hz) techniques, and the Cr-thickness-dependent measurements were dc. The measurements were taken by incrementing **H** from +20 kG to −20 kG then back to +20 kG, as shown in Fig. 2.

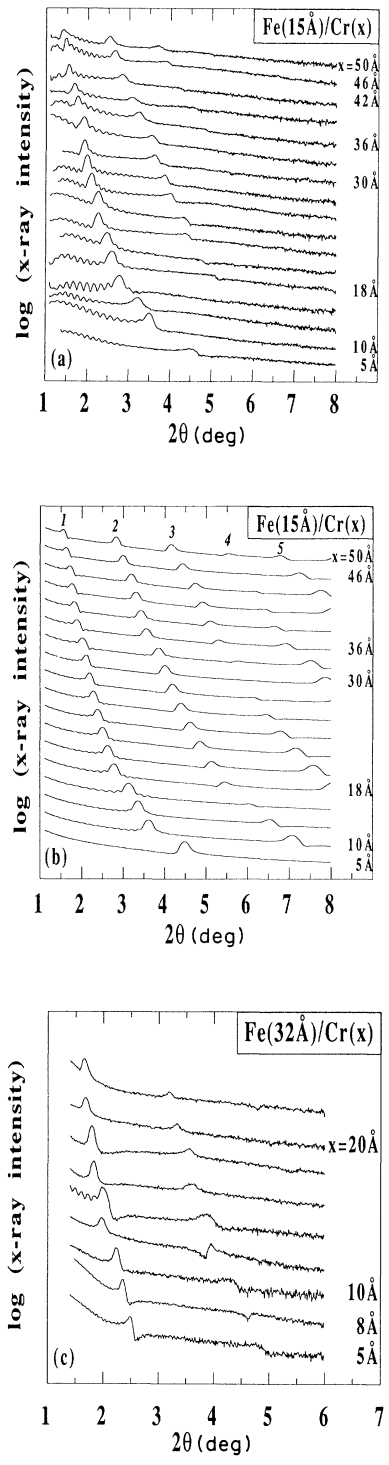

FIG. 1. Low-angle, Cu $K\alpha$ x-ray-diffraction results for Fe/Cr superlattices. (a) is experimental and (b) is a dynamical simulation for Fe (15 Å)/Cr(x). Results for each film are shifted vertically for clarity. In the unlabeled spectra the thickness x is incremented by 2 Å or Cr for successive films. As many as five orders of diffraction peaks appear in (b), while fewer are observed in (a) due to interfacial mixing. (c) shows experimental results for Fe(32 Å)/Cr(x) superlattices.

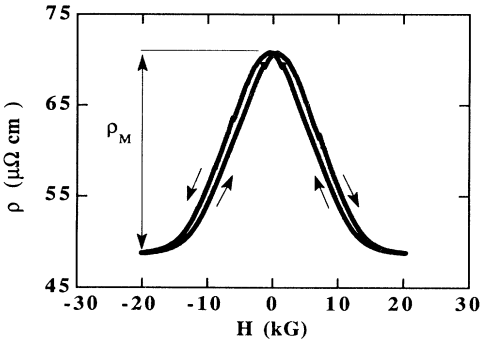

FIG. 2. Resistivity of [Fe(15 Å)/Cr(11 Å)]$_{20}$ at 4.2 K showing the giant magnetoresistivity contribution denoted ρ_M.

III. RESULTS

A. Magneto-optic Kerr rotation

The longitudinal Kerr-rotation Φ_K results at room temperature are shown in Fig. 3. The bold curve is calculated from the formalism of Zak *et al.*[12] utilizing the tabulated optical constants[13] for bulk Fe and Cr, and published magneto-optical constants for Fe.[14] (The scale factor of 0.7 in the calculations is similar to that found in other studies.[15]) It is apparent from the data in Fig. 3 that the rotation agrees with the calculated values in the saturation state for the ferromagnetically aligned films. Unfortunately, the saturation values of Φ_K for the AF-coupled films are not accessible because of the low fields available for Kerr-rotation measurements ($\sim$2 kG) compared to the high saturation field $\mathbf{H}_{\rm sat}$ ($\sim$5 kG) needed. Measurements of the Kerr rotation as determined from the remnant state show quite clearly that the AF films have a large departure from the calculated trend. Thus, we use this departure to delineate the region of antiparallel coupling between the layers. The higher-order AF oscillations are not apparent, although they are clearly present in the MR at 77 K, as we will see in the next section. This is partially because it is more favorable to observe weak oscillations in the MR due to the enhanced sensitivity and the lower temperature of the transport measurements. The higher-order oscillations dampen in the MR measurements because of the mean free path of the conduction electrons. In the Kerr-rotation results the origin of the dampening of the higher-order oscillations is different. The characteristic length scale is the depth penetration of the light compared to the bilayer thickness. As the bilayer thickens the light eventually will enter only the top ferromagnetic layer in the stack, but that limit ($\sim$200 Å) is not reached in our films. The washing out of the higher-order oscillations in the Kerr-rotation measurements may be due to structural imperfections.

B. Magnetoresistivity versus Cr thickness

Figure 2 shows the resistivity versus **H** at 4.2 K for a representative AF film. The definition of $\rho_{\rm M}$ appears in the figure as:

$$\rho_{\rm M}(T,\mathbf{H})=\rho(T,\mathbf{H}=0)-\rho(T,\mathbf{H}),$$

where the $\rho(T,\mathbf{H})$ are measured quantities. The definition applies to any sample, regardless of the coupling, at any T. The magnitude of the MR ratio, traditionally reported as a percentage value, is the normalized quantity $\rho_M(T,\mathbf{H}_{\rm sat})/\rho(T,\mathbf{H}_{\rm sat})$, which we will abbreviate simply as $\rho_M/\rho_{\rm sat}$. The MR ratio at 77 K appears plotted in Fig. 4 as a function of Cr thickness, and it shows the same oscillations that were observed by Parkin, More, and Roche.[3] The oscillations in Fig. 4 are directly related to the type of coupling between the Fe layers; large values of the MR ratio are associated with AF-coupling between Fe layers and are centered at $\sim$12, 27, and 42 Å Cr thickness. The straight line through the AF peaks illustrate that the dampening of the MR discussed in Sec.

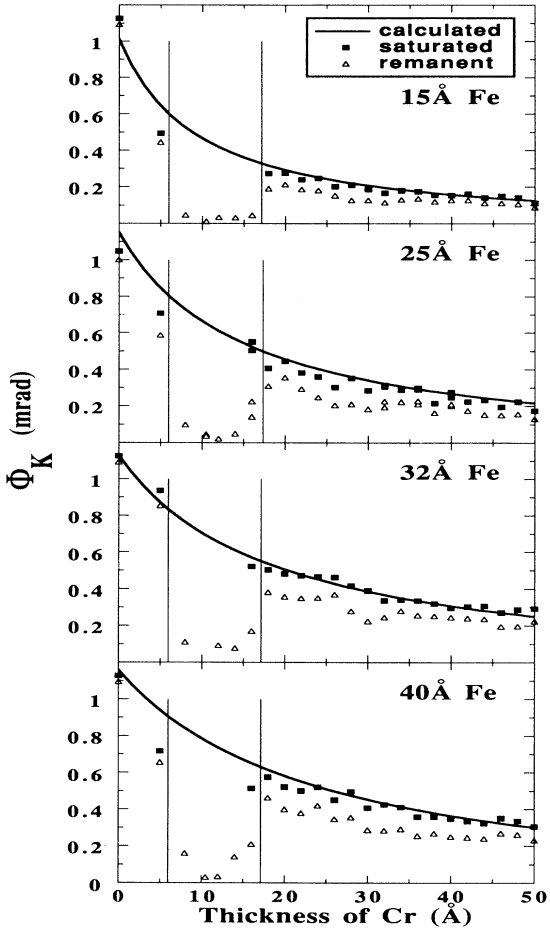

FIG. 3. Kerr rotation for Fe/Cr superlattices using *p*-polarized He-Ne light. The solid curves are calculated and scaled by a factor of 0.7; the open (closed) symbols are obtained from remnant (saturation-) state Kerr-intensity measurements. The measurements that agree with the calculations are for ferromagnetically-aligned films. Most AF films between $\sim$6 and 17 Å Cr, as delineated by the straight lines, could not be saturated.

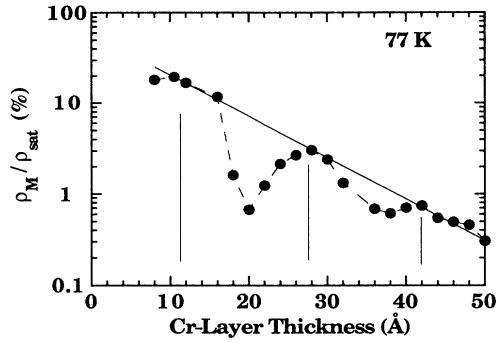

FIG. 4. Normalized magnetoresistivity of Fe(32 Å)/Cr superlattices at 77 K showing the exponential dampening of the three AF peaks, which are denoted by vertical lines. The dashed curve is a guide to the eye.

III A is exponential, as has also been reported by Barthélémy *et al.*[16] Figure 5 isolates the numerator and denominator of ρ_M/ρ_{sat} into separate panels to show that the oscillations in Fig. 4 are due to the behavior of ρ_M and not that of ρ_{sat}, which is relatively constant.

It has been shown by Wang, Levy, and Fry[8] that application of RKKY-coupling theory to films with perfect interfaces leads to small-period oscillations ($\sim$2–4 Å), whereas the observed oscillations typically have periods of $\sim$10–20 Å. Wang, Levy, and Fry[8] also have shown that the existence of roughness at the interface gives rise to oscillations with a period of $\sim$20 Å due. Thus, such a modified RKKY interaction is, in general, consistent with the observed oscillations between AF and ferromagnetic coupling in these films.

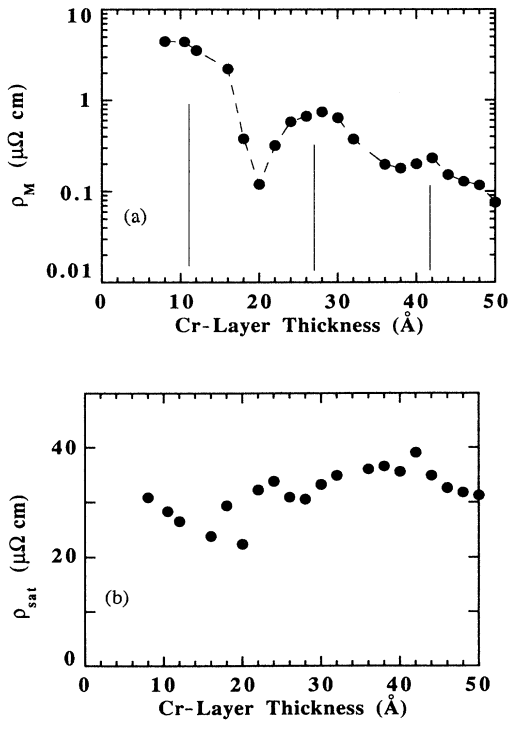

FIG. 5. Resistivity contributions for Fe(32 Å)/Cr superlattices at 77 K. The numerator of the quantity plotted in Fig. 4 appears in (a) and the denominator in (b).

C. Temperature dependence of the magnetoresistivity

The major features of the magnetic-field behavior of the resistivity in these films are reproduced quite well by the theory of Camley and Barnas.[9] However, in order to account for the change in the magnitude of the MR ratio between 4 and 300 K, these authors required a change in the mean free path of the conduction electrons of nearly two orders of magnitude. This is in apparent disagreement with the observed residual-resistance ratio (RRR), defined as $\rho(300\ \mathrm{K})/\rho(4\ \mathrm{K})$, values of which appear in Table I. To try to understand this issue better we have measured the MR as a function of T for two AF films. We have also measured one ferromagnetic film on a courser T grid for comparison purposes. The ferromagnetic films have a much smaller MR than the AF films, as is apparent in Fig. 4. Before discussing the results, we need to first determine the proper way to express then so as to separate the T-dependent effects of the MR from the effects of the variation of the mean free path and from impurity and grain-boundary scattering. We approximate the resistivity as[17]

$$\rho(T,\mathbf{H})=\rho_0+\rho_{sd}(T)+\rho_M(T,\mathbf{H})\ , \tag{1}$$

where $\rho(T,\mathbf{H})$ is the measured resistivity, ρ_0 is the constant resistivity due to grain boundary and impurity scattering (in practice this is defined as the resistivity at 4 K and above the saturation field), ρ_{sd} includes the *s-d* interband scattering mediated by both phonons and magnons, and ρ_M is the MR as discussed above. We assume that the magnetic-field dependence of the resistance due to grain boundaries and standard Lorentz scattering is negligible, which is justified since the RRR is low. In Fig. 6 we plot ρ_M/ρ_{sat} versus T for a representative sample and observe that it saturates to a maximum value at low T, as has been reported previously.[16] For the purposes of our analysis we study the T dependence of the magnetic scattering in this system by comparing the

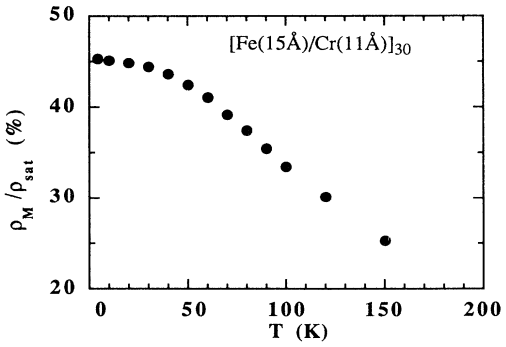

FIG. 6. Normalized magnetoresistivity of an [Fe(15 Å)/Cr(11 Å)]$_{30}$ superlattice as a function of temperature.

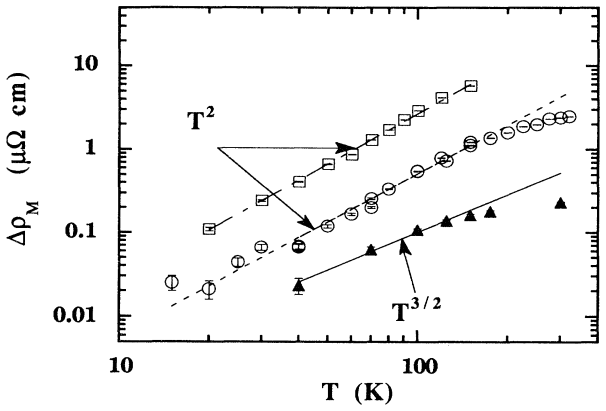

FIG. 7. log-log plots of the quantity $\Delta\rho_M$ vs T for AF films (open symbols) and ferromagnetic film (closed triangle symbol) showing T_2 and $T^{3/2}$ straight-line behaviors, respectively, attributed to the thermal excitation of magnons. The films are described in Table I. The square symbols are for the 15-Å Fe film, and the circles are for the 32-Å Fe film.

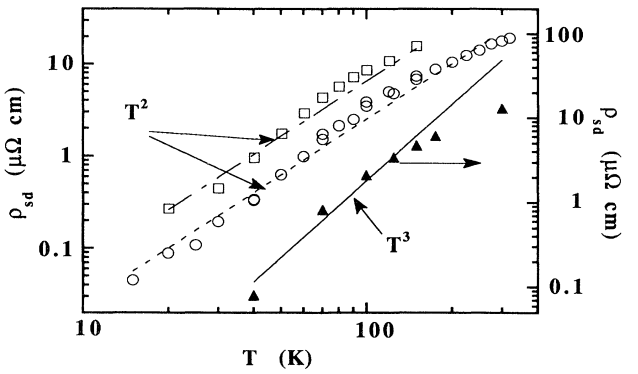

FIG. 8. log-log plots of ρ_{ds} vs T for the same films and using the same symbols as in Fig. 7. The T^2 and T^3 straight-line behaviors are attributed to magnon- and phonon-assisted scattering processes, respectively.

difference between $\rho_M(T)$ and its maximum value at $T=0$:

$$\Delta\rho_M(T)=\rho_M(T=0)-\rho_M(T)\ .$$

Figure 7 shows a log-log plot of the quantity $\Delta\rho_M$ versus T. The slope of the log-log plot yields the exponent n in the relationship $\Delta\rho_M \propto T^n$. If the value of n at low T takes on an integer or half-integer value, we regard this as defining a power law that serves as a hint of the underlying scattering mechanism. Figure 7 shows that the AF-coupled films follow a T^2 behavior at low T (over a range of a factor of 10 in temperature), and that the ferromagnetic film can be approximated by a $T^{3/2}$ behavior. If the resistivity decomposition depicted by Eq. (1) is realistic, then log-log plots of the quantity $\rho_{sd}=\rho(t)-\rho_0-\rho_M(T,\mathbf{H})$ versus T for each sample should also yield tractable slopes. Figure 8 shows such plots. The ferromagnetic sample can be approximated roughly by a T^3 behavior, while the AF films show T^2 behavior. The significance of the various T dependences analyzed in this subsection are discussed in Sec. IV.

IV. DISCUSSION

A. Magnetoresistivity

The recent theories explaining the origin of giant MR treat the boundary-scattering problem by invoking phenomenological transmission and reflection probabilities.[9] The conduction electrons are scattered at the ferromagnetic-nonferromagnetic interface with different transmission (and reflection) coefficients depending on whether their spin is parallel or antiparallel to the direction of the magnetization of the ferromagnetic layer. In ferromagnetically-aligned samples, the conduction electrons that are polarized parallel to the majority-spin direction of the magnetized Fe layer shunt the current and yield a low resistivity.[2] This is contrasted with AF samples where the conduction electrons of both spin orientations encounter alternate interfaces that have high scattering probability. This leads to a higher resistivity than for the ferromagnetic films and serves as a basis for the change in resistivity observed in Fig. 2.

We assume that the observed reduction of ρ_M at finite T, compared with its value at $T=0$, is a consequence of the thermal excitation of magnons which cause local spin disordering in the magnetic layers. Then, to first-order approximation, we can write

$$\Delta\rho_M(T)\propto\langle n\rangle_T\ , \tag{2}$$

where $\langle n\rangle_T$ is the magnon occupation number at a given temperature, which is obtained from the integral of the magnon dispersion relation with the Bose-Einstein statistical factor. If our assumption is correct, the $\Delta\rho_M(T)$ and $\langle n\rangle_T$ should yield the same T dependence.

It is well known that the $\langle n\rangle_T$ for a three-dimensional (3D) ferromagnet obeys a $T^{3/2}$ law at temperatures well below the Curie temperature T_C, i.e.,

$$\langle n\rangle_{T_{\text{ferro}}}\propto T^{3/2}\ . \tag{3}$$

TABLE I. Description of the films used in the temperature-dependent studies.

Film	[Fe(32 Å)/Cr(20 Å)]$_{30}$	[Fe(32 Å)/Cr(11 Å)]$_{30}$	[Fe(15 Å)/Cr(11 Å)]$_{20}$
Coupling	Ferromagnetic	AF	AF
ρ_0 ($\mu\Omega$ cm)	21.8	22.4	48.6
RRR	1.6	1.5	$\gtrsim 1$
$\rho_M(T=4$ K) ($\mu\Omega$ cm)	0.28	5.0	22.0

Our ferromagnetic superlattice, which has a number of quasi-2D ferromagnetic sheets coupled ferromagnetically, is equivalent to an anisotropic 3D ferromagnet. Therefore, a $T^{3/2}$ law is expected for $\langle n \rangle_T$ at low T. Our measurements are reported above 20 K due to sensitivity considerations, however, it is possible that there is a minimum wave-vector requirement on the scattering process that would put a lower bound on the T range of validity of expression (2). A similar expression to (3) for the 3D AF case would be $\langle n \rangle_{T_{\rm AF}} \alpha T^3$, however, it has recently been shown[18] that for *anisotropic* AF materials the magnon dispersion relation is modified such that, at low T,

$$\langle n \rangle_{T_{\rm AF}} \propto T^2 \ . \tag{4}$$

Singh *et al.*[18] have explored this regime theoretically; they have also experimentally confirmed the T^2 law in Mössbauer measurements of the magnetization of the AF insulator La_2CuO_4 the precursor to the famous high-temperature superconducting compound, where they substitutionally replaced a small percentage of the moment-carrying Cu sites with an Fe Mössbauer nucleus. The structure of the cuprate consists of weakly-coupled Cu-O_2 layers, but the in-plane coupling as well as the interplanar coupling is AF, and the Cu-O_2 layers are of atomic thickness. Our Fe/Cr superlattices also consist of weakly coupled layers, but the in-plane coupling is ferromagnetic. Qiu *et al.*[19] have calculated $\langle n \rangle_T$ at low T for weakly AF-coupled 2D *ferromagnetic* sheets, based on a Heisenberg model, and find that the T^2 law of expression (4) persists. This is in closer analogy to the situation of our interest, except that the ferromagnetic sheets are constrained in the derivation to be of atomic thickness. Another point that should be mentioned is that it is also possible that the integrations to yield $\langle n \rangle_T$ in expressions (3) and (4) should contain transport matrix elements that assign more weight to certain magnon excitations than to others. Zhang, Levy, and Fert[20] have recently explored this possibility using a single localized mode to interpret the unpublished MR data of Petroff *et al.*[21] Since we only are interested in the leading T dependence of $\langle n \rangle_T$, we ignore weighting factors, but note that a continuum spectrum is necessary, as will be amplified at the end of this section. The agreement obtained between the temperature dependencies of $\langle n \rangle_T$ and $\Delta\rho_M$ is quite striking. It provides support that thermal excitation of magnons plays an important role in governing the T dependence of the MR.

B. *s-d* interband resistivity

Further support that our approach provides valuable insights comes from the analysis of the approximate T dependences of the ρ_{sd} resistivity contribution. We have observed from the results of Fig. 8 that ρ_{sd} for the ferromagnetic film can be roughly approximated by a T^3 behavior. T^3 is expected at low T for transition metals from phonon scattering.[22] Of course, the T range over which such behavior is expected to apply is reduced compared to that for magnon scattering, because the characteristic scale is set by the Debye temperature, which is on the order of 3-times lower than T_C. For the AF films ρ_{sd} is dominated by a T^2 term over a relatively broad T range (see Fig. 8). This suggests that magnon-assisted scattering[23–24] adds to the phonon contribution to ρ_{sd} for the AF films. The phonon contribution to ρ_{sd} should be similar in both ferromagnetic and AF films.

It should be mentioned that a T^2-resistivity contribution at low T is well known to also arise from electron-electron scattering[26,27] (e.g., spin fluctuations, Baber scattering, etc.). However, we interpret the T^2 contribution as arising from magnon-assisted *s-d* interband scattering because the T^2 term in our films is uniquely associated with the AF state.

It is important to discuss the relationship of our work to the recent study of Zhang, Levy, and Fert[20] on the t dependence of ρ_M. We are in agreement with their general conclusion that magnetic excitations are responsible for the behavior of $\rho_M(T)$. However, those authors made a simplifying assumption that emphasizes the role of a single, local excitation, while our analysis indicates that a continuous magnon excitation spectrum underlies our results. Thus, the present work rules out the simplification of an Einstein-type spectrum for the interfacial magnons.

V. SUMMARY

We have examined the system Fe/Cr and performed magneto-optical and MR measurements. The magneto-optics serves as a convenient probe of the magnetic coupling of these systems. We have confirmed the oscillatory behavior of the MR reported by Parkin, More, and Roche[3] for sputtered Fe/Cr superlattices. The MR shows three oscillations due to AF coupling. The magnitude of the AF MR anomaly decreases exponentially with increasing Cr thickness. We systematically explored the T dependence of the MR for three samples, two AF and one ferromagnetic, and find T^2 and $T^{3/2}$ power laws at low T, respectively, which we attribute to the thermal excitation of magnons. Thus, the thermal excitation of magnons simultaneously decreases ρ_M and increases ρ_{sd} as T increases. Hence, there appears to be a spillover from the ρ_M channel to the magnon-assisted ρ_{sd} channel as T increases.

From our study we can make the following two general statements about the MR: (1) the T dependence of the ρ_M is primarily determined by the thermal excitation of magnons and is not due to a mean free path of the conduction electrons that changes dramatically with temperature, and (2) it is more illuminating to express the MR as we have defined ρ_M, rather than in the conventional manner using the normalized quantity $\rho_M/\rho_{\rm sat}$.

ACKNOWLEDGMENTS

This work was supported by the U.S. Department of Energy, BES–Materials Sciences under Contract No. W-31-109-ENG-38. We thank G. Felcher for the use of his

reflectivity code to calculate the low-angle x-ray diffraction of our superlattices. We also thank P. Levy for sending a copy of work prior to publication. One of us (J.E.M.) was supported by the NSF Materials Research Group, Contract No. DMR-86-03304 at the University of Texas, Austin.

[1]P. Grüberg, R. Schreiber, Y. Pang, M. B. Brodsky, and C. H. Sowers, Phys. Rev. Lett. **57**, 2442 (1986).

[2]M. N. Baibich, J. M. Broto, A. Fert, F. Nguyen Van Dau, F. Petroff, P. Etienne, G. Creuzet, A. Friederich, and J. Chazelas, Phys. Rev. Lett. **61**, 2472 (1988)

[3]S. S. P. Parkin, N. More, and K. P. Roche, Phys. Rev. Lett. **64**, 2304 (1990).

[4]B. Heinrich, Z. Celinski, J. F. Cochran, W. B. Muir, J. Rudd, Q. M. Zhong, A. S. Arrot, K. Myrtle, and J. Kirschner, Phys. Rev. Lett. **64**, 673 (1990).

[5]W. R. Bennett, W. Schwartzacher, and W. F. Egelhoff, Jr., Phys. Rev. Lett. **65**, 3169 (1990).

[6]S. Pescia, D. Kerkmann, F. Schumann, and W. Gudat, Z. Phys. B **78**, 475 (1990); A. Cebollada, R. Miranda, C. M. Schneider, P. Shuster, and J. Kirschner (unpublished); D. H. Mosaca, F. Petroff, A. Fert, P. A. Schroeder, W. P. Pratt, Jr., R. Laloee, and S. Lequien, J. Magn. Magn. Mater. **94**, L1 (1991); S. S. P. Parkin, R. Bhadra, and K. P. Roche, Phys. Rev. Lett. **66**, 2152 (1991).

[7]M. E. Brubaker, J. E. Mattson, C. H. Sowers, and S. D. Bader, Appl. Phys. Lett. **58**, 2306 (1991).

[8]Y. Wang, P. M. Levy, and J. L. Fry, Phys. Rev. Lett. **65**, 2732 (1990); W. Baltensperger and J. S. Helman, Appl. Phys. Lett. **57**, 2954 (1990); H. Hasegawa, Phys. Rev. B **42**, 2368 (1990).

[9]R. E. Camley and J. Barnas, Phys. Rev. Lett. **63**, 664 (1989).

[10]P. M. Levy, S. Zhang, and A. Fert, Phys. Rev. Lett. **65**, 1643 (1990).

[11]Mahbub R. Kahn, C. S. L. Chun, G. P. Felcher, M. Grimsditch, A. Kueny, Charles M. Falco, and Ivan K. Shuller, Phys. Rev. B **27**, 7186 (1983); M. Piecuch and L. Nevot, Mater. Sci. Forum **59** and **60**, 93 (1990), Sec. 4.2 is particularly pertinent to this analysis.

[12]J. Zak, E. R. Moog, C. Liu, and S. D. Bader, J. Magn. Magn. Mater. **89**, 107 (1990).

[13]*CRC Handbook of Chemistry and Physics,* 71st ed., edited by David R. Lide (CRC, Boca Raton, 1990).

[14]G. S. Krinchik and V. A. Artem'ev, Zh. Eksp. Teor. Fiz. **53**, 1901 (1967) [Sov. Phys. JETP **26**, 1080 (1968)].

[15]E. R. Moog, S. D. Bader, and J. Zak, Appl. Phys. Lett. **56**, 2687 (1990).

[16]A. Barthélémy, A. Fert, M. N. Baibich, S. Hadjoudj, F. Petroff, P. Etienne, R. Cabanel, S. Lequien, F. Nguyen Van Dau, and G. Creuzet, J. Appl. Phys. **67**, 5908 (1990).

[17]J. E. Mattson, Ph.D. thesis, Northwestern University, 1990. In this work a similar decomposition was shown to provide helpful insight toward understanding the temperature dependence of the magnetoresistance in thin Cr films.

[18]A. Singh, Z. Tesanovic, H. Tang, G. Xiao, C. L. Chien, and J. C. Walker, Phys. Rev. Lett. **64**, 2571 (1990).

[19]Z. Q. Qiu, J. E. Mattson, C. H. Sowers, V. Welp, S. D. Bader, H. Tang, and J. C. Walker (unpublished).

[20]S. Zhang and P. M. Levy, Phys. Rev. B **43**, 11 048 (1991).

[21]F. Petroff, A. Barthélémy. A. Hamzic, A. Fert, P. Etienne, S. Lequien, and G. Creuzet, J. Magn. Magn. Mater. **93**, 95 (1991).

[22]A. H. Wilson, Proc. R. Soc. London, Ser. A **167**, 580 (1938); A. H. Wilson, *Theory of Metals* (Cambridge University, Cambridge, 1954); see also S. D. Bader and F. Y. Fradin, *Superconductivity in d- and f-Band Metals* (Plenum, New York, 1976), p. 567.

[23]T. Kasuya, Prog. Theor. Phys. (Kyoto) **16**, 58 (1956); **22**, 227 (1956).

[24]D. A. Goodings, Phys. Rev. **132**, 542 (1963).

[25]George Terence Meaden, *Electrical Resistance of Metals* (Plenum, New York, 1965).

[26]M. B. Brodsky, A. J. Arko, A. R. Harvey, and W. J. Nellis, in *The Actinides: Electronic Structure and Related Properties,* edited by A. J. Freeman and J. B. Darby, Jr. (Academic, New York, 1974), Vol. 2, p. 186.

[27]S. Doniach, in *The Actinides: Electronic Structure and Related Properties* (Ref. 26), p. 51.